Soils and Foundations 2013;53(5):692–707

The Japanese Geotechnical Society

Soils and Foundations

www.sciencedirect.com
journal homepage: www.elsevier.com/locate/sandf

Seismic uplift capacity of shallow horizontal strip anchor under oblique load using pseudo-dynamic approach

Sunil M. Rangari, Deepankar Choudhury*, D.M. Dewaikar

Department of Civil Engineering, Indian Institute of Technology (IIT) Bombay, Powai, Mumbai 400076, India

Received 11 January 2012; received in revised form 17 May 2013; accepted 18 June 2013
Available online 24 September 2013

Abstract

In this paper, an analytical method to compute the uplift capacity of an obliquely loaded horizontal strip anchor under both static and seismic conditions is described using the limit equilibrium method. The distribution of the soil reactions on a simple planar failure surface is obtained through the use of Kötter's equation, and the pseudo-dynamic approach is used to obtain the net seismic vertical uplift capacity factor for the unit weight component of the soil ($F_{\gamma d}$). The results for the static and seismic vertical uplift capacity factors are determined for various combinations of input parameters, such as the load inclination, the soil friction angle, the embedment ratio, the soil amplification and both horizontal and vertical pseudo-dynamic seismic accelerations. It is observed that the orientation of the load significantly affects the seismic uplift capacity of the horizontal strip anchor. $F_{\gamma d}$ is seen to decrease with an increase in both horizontal and vertical seismic accelerations and soil amplification, whereas it is seen to increase with an increase in the embedment ratio and the soil friction angle, as expected. The results in terms of the non-dimensional net seismic uplift capacity factor are presented in graphical and tabular forms. The present results are compared and found to be in good agreement with similar results available in literature.

Keywords: Horizontal strip anchor; Kötter's equation; Oblique load; Limit equilibrium method; Pseudo-dynamic approach; Soil amplification; Seismic uplift capacity; Closed-form analytical solution

1. Introduction

Ground anchors are commonly used as foundation systems for important structures requiring uplift resistance, such as transmission towers, pipe lines buried under water, sheet pile walls, etc. It is well known that horizontal anchors are subjected to the vertical uplift load, and that when it reaches the ultimate load condition, failure surfaces develop around the anchor plate. These failure surfaces reach the ground surface for shallow anchors. The problem becomes more complex and important under seismic conditions due to the devastating nature of earthquake forces on such ground anchors. The importance of the computation of the vertical uplift capacity of horizontal ground anchors is clear; it is an important topic for geotechnical engineers to address, under both static and seismic conditions. Hence, the effect of earthquakes on the uplift capacity of a strip anchor is studied in the present theory, as this knowledge is vital to the study of the behavior of strip anchors under seismic conditions.

For static conditions, numerical solutions for the uplift capacity of horizontal anchors were obtained using the limit equilibrium method (Vesic, 1971; Meyerhof and Adams, 1968). The finite element method was used with a limit analysis to

*Corresponding author. Tel.: +91 22 2576 7335 (office), +91 22 2576 8335 (residence); fax: +91 22 2576 7302, +91 22 2572 3480.
E-mail addresses: dc@civil.iitb.ac.in (D. Choudhury), dmde@civil.iitb.ac.in (D.M. Dewaikar).
Peer review under responsibility of The Japanese Geotechnical Society.

Production and hosting by Elsevier

0038-0806 © 2013 The Japanese Geotechnical Society. Production and hosting by Elsevier B.V. All rights reserved.
http://dx.doi.org/10.1016/j.sandf.2013.08.007

compute the uplift capacity of anchors (Kumar and Kouzer, 2008; Merifield and Sloan, 2006; Tagaya et al., 1983). Experimental results and analytical solutions were obtained using the limit equilibrium method and a limit analysis (Rowe and Davis, 1982; Murray and Geddes, 1987; Tagaya et al., 1988; Dickin and Laman, 2007). Analytical models were presented by some researchers (Chattopadhayay and Pise, 1986; Deshmukh et al., 2011), whereas Kumar (1999) and Subba Rao and Kumar (1994) used an upper bound limit analysis to predict the pullout capacity of ground anchors, and Honda et al. (2011) employed a two-dimensional distinct element analysis to obtain the uplift capacity of belled and multi-belled piles in sand. Series of centrifuge tests were presented by Hugo et al. (2010) to determine the effect of gapping on the uplift capacity of a shallow skirted foundation. Miyata et al. (2011) obtained the accuracy of a single square anchor plate for obtaining the capacity in a multi-anchor wall system by applying two models.

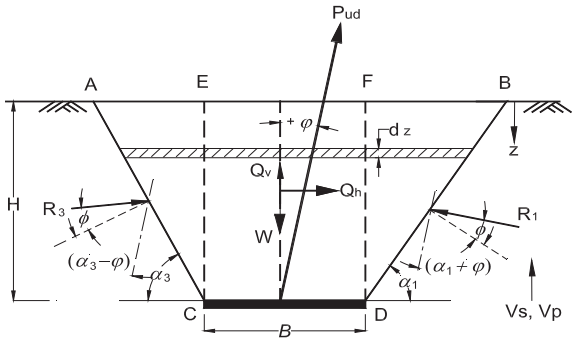

Fig. 1. The typical model considered under seismic conditions.

Few researchers have obtained the vertical uplift capacity of horizontal plate anchors under seismic conditions (Kumar, 2001; Choudhury and Subba Rao, 2004; Rangari et al., 2011a).

Based on field and laboratory tests, a semi-empirical relation was developed for the breakout resistance of a horizontal strip anchor under an oblique load by Meyerhof (1973). Das and Seeley (1975), on the other hand, obtained model test results for a square anchor in dry sand subjected to inclined loads and presented in graphical form.

A pseudo-dynamic approach, developed by Steedman and Zeng (1990) and upgraded by Choudhury and Nimbalkar (2005), was used by Ghosh (2009) to obtain the seismic uplift capacity of a horizontal plate anchor by considering the effect of seismic amplification using an upper bound limit analysis and assuming a simple planar failure surface.

In a pseudo-static analysis, the dynamic loading induced by an earthquake is considered as time-independent, which ultimately assumes that the magnitude and the phase of the acceleration are uniform throughout the depth of the soil layer. Also, in a pseudo-static analysis, the effect of the amplification of vibrations cannot be considered; this effect generally occurs towards the ground surface and depends on various soil parameters, such as damping and the shear modulus of the soil (Steedman and Zeng, 1990). Rectifying these shortcomings of the pseudo-static approach, Steedman and Zeng (1990) proposed a pseudo-dynamic approach, which considers the effect of the finite shear wave velocity, horizontal seismic acceleration and the amplification of vibrations, to obtain the active earth pressure on retaining walls for a particular value of soil friction angle. Later, Choudhury and Nimbalkar (2005) modified the approach further to consider the effect of vertical acceleration also due to vertically propagating primary waves along with horizontal seismic acceleration; they

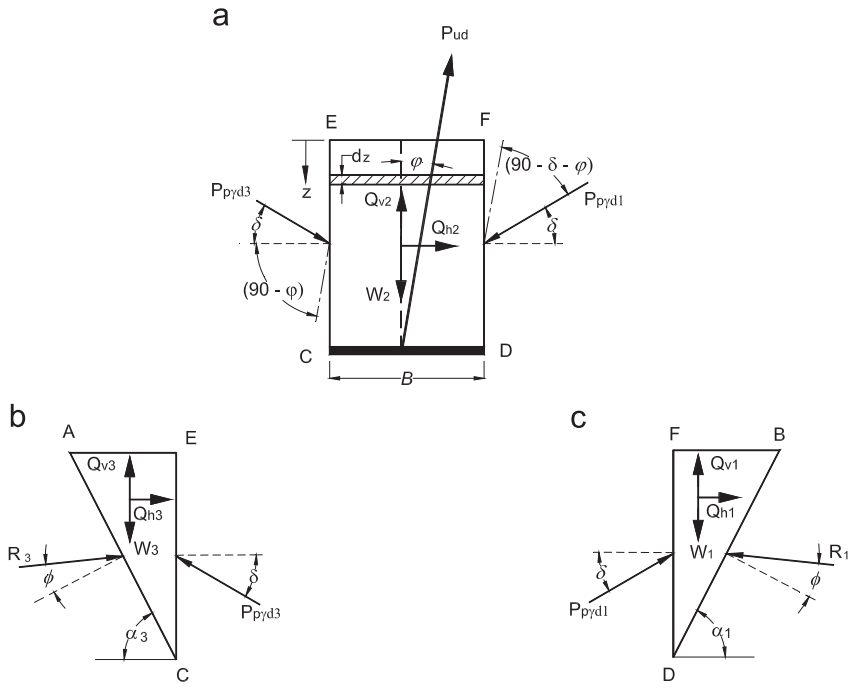

Fig. 2. Free body diagram with various forces on failure wedges.

considered the effects of time, the phase difference and the effect of amplification in both shear and primary waves propagating through the soil.

Kötter (1903) was used by researchers (Balla, 1961; Matsuo, 1967, 1968) to obtain the soil resistance on the failure surface. Recently, the limit equilibrium method has been effectively applied along with Kötter's equation to obtain the vertical uplift capacity of horizontal strip anchors (Deshmukh et al., 2011; Rangari et al., 2011a). However, the use of Kötter (1903) for obtaining the seismic uplift capacity of horizontal strip anchors under an oblique load is still scarce in literature and remains mostly unnoticed.

Hence, in this paper, an attempt has been made to obtain the uplift capacity of a horizontal strip anchor under both static and seismic conditions by employing Kötter's equation (1903) and by taking the forces on the soil column above the anchor into consideration. It is well known that the problem of the computation of the seismic uplift capacity of horizontal strip anchors is the application of the seismic passive resistance on retaining walls for the negative wall friction condition (Choudhury and Subba Rao, 2002, 2005a; Rangari et al., 2013), whereas the case of the positive wall friction condition is used for bearing capacity analyses (Subba Rao and Choudhury, 2005; Choudhury and Subba Rao, 2005b). A pseudo-dynamic approach is used with the limit equilibrium method for a simple planer failure surface to obtain the seismic uplift capacity of an anchor with negative wall friction angle $\delta=2\phi/3$ (Meyerhof and Adams, 1968; Choudhury and Subba Rao, 2004; Rangari et al., 2011a, 2011b, 2013), where ϕ is the soil friction angle.

2. Method of analysis

The net seismic uplift capacity factor for a shallow horizontal strip anchor, subjected to an inclined load, is obtained using the limit equilibrium method and assuming a simple planar failure

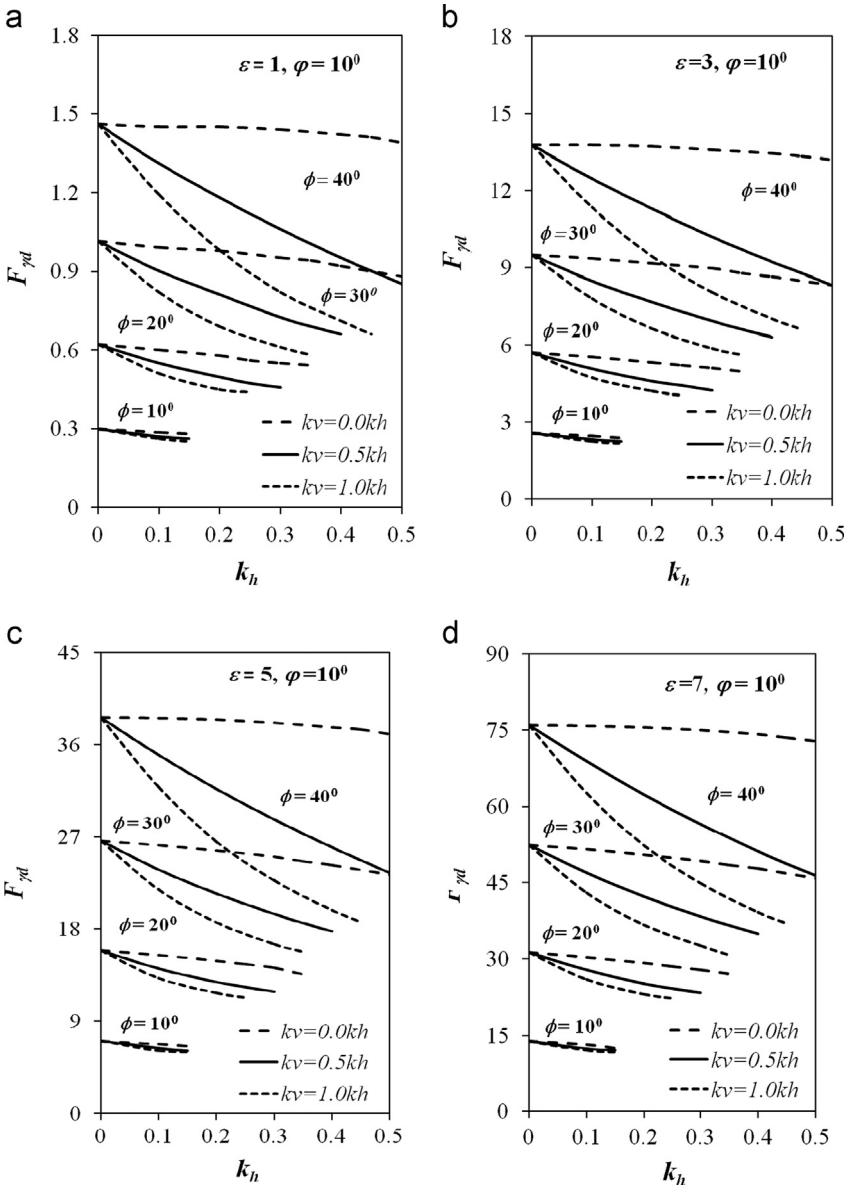

Fig. 3. Variation in $F_{\gamma d}$ for various values of k_h and k_v for $\varphi=+10^\circ$ for (a) $\varepsilon=1$, (b) $\varepsilon=3$, (c) $\varepsilon=5$ and (a) $\varepsilon=7$ with $f=1.0$, $H/\lambda=0.3$ and $H/\eta=0.16$.

surface and a pseudo-dynamic approach for seismic forces. The soil is assumed as a rigid cohesionless material satisfying the Mohr–Coulomb failure criterion. It is assumed that the input values for the soil parameters, such as unit weight γ and soil friction angle ϕ, are not affected under seismic conditions. The smooth anchor plate is considered by disregarding its mass in the analysis. The marginal effect ($<4\%$) of the roughness of the plate anchor on the calculated uplift capacity of a shallow horizontal strip anchor for all soil friction angles and embedment ratios was observed by Merifield and Sloan (2006); it justifies the assumption of the smooth anchor plate used in the present study. It is also assumed that the soil lying below the surface of the anchor does not offer any resistance to the uplift capacity.

Fig. 1 shows the model considered for the horizontal plate anchor with an oblique load under seismic conditions. A horizontal plate anchor (CD) of width B is embedded at a depth H from the horizontal ground surface. W is the weight of failure wedge ACDB, R_1 and R_3 are the reactions on planar failure surfaces BD and AC, respectively, and Q_h and Q_v are the horizontal and vertical inertia forces acting in horizontal and vertical directions, respectively.

Kötter's equation (1903) for the passive state of earth pressure in a cohesionless soil is employed to obtain the distribution of soil reactions on a curved surface and can be expressed as

$$\frac{dp}{ds}+2p\ \tan\ \phi\ \frac{d\alpha}{ds}=\gamma\ \sin(\alpha+\phi) \tag{1}$$

where

dp = differential reaction pressure on failure surface
ds = differential length of failure surface
ϕ = soil friction angle

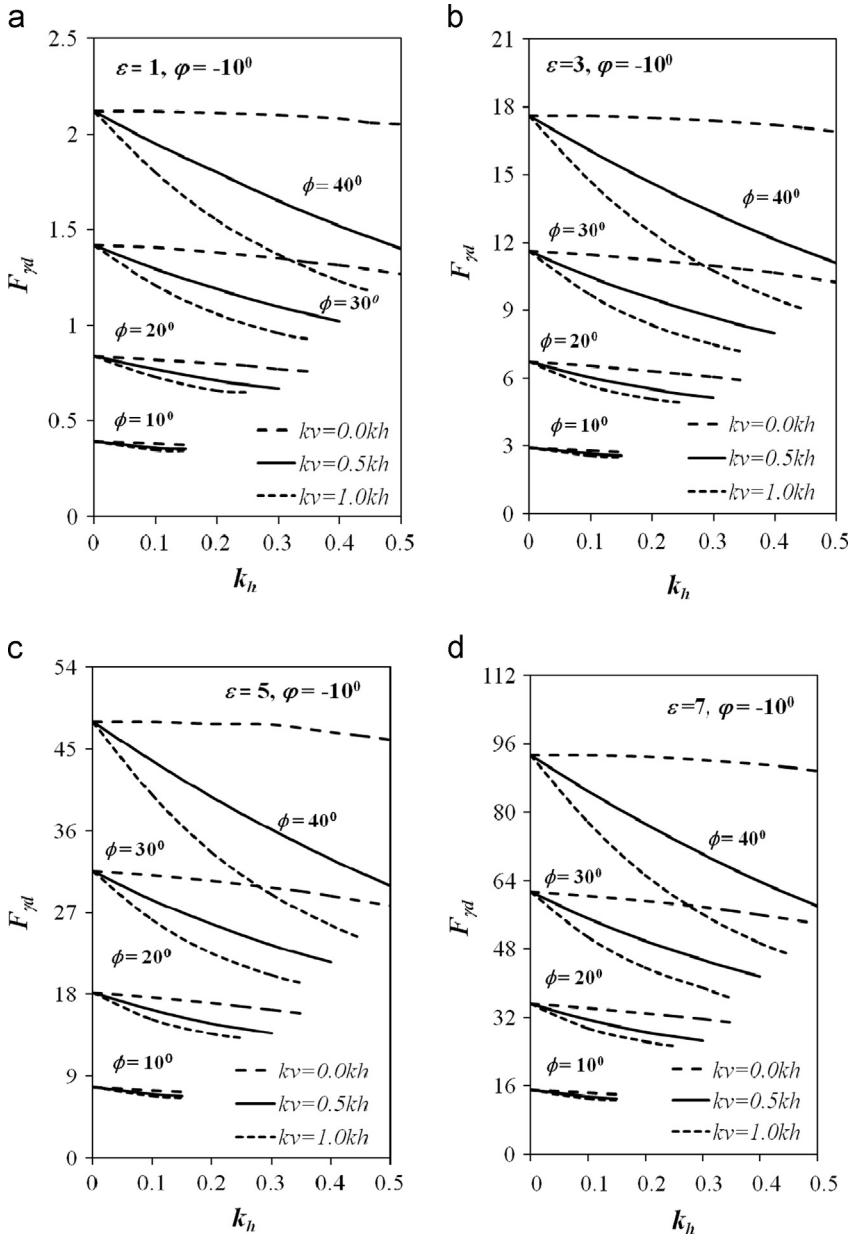

Fig. 4. Variation in $F_{\gamma d}$ for various values of k_h and k_v for $\varphi=-10^\circ$ for (a) $\varepsilon=1$, (b) $\varepsilon=3$, (c) $\varepsilon=5$ and (a) $\varepsilon=7$ with $f=1.0$, $H/\lambda=0.3$ and $H/\eta=0.16$.

$d\alpha$ = differential angle
γ = unit weight of soil
α = inclination of tangent on failure surface at point of interest with horizontal.

Integrating Eq. (1) and using the boundary conditions on failure surfaces BD and AC, reactions R_1 and R_3 can be obtained as follows (Rangari et al., 2011a):

$$R_1 = \frac{1}{2}\frac{\gamma H^2 \sin(\alpha_1+\phi)}{\sin^2\alpha_1} \quad (2)$$

$$R_3 = \frac{1}{2}\frac{\gamma H^2 \sin(\alpha_3+\phi)}{\sin^2\alpha_3} \quad (3)$$

Failure wedge ACDB, shown in Fig. 1, under the pseudo-dynamic approach, considers the propagation of finite shear wave velocity $V_s = \sqrt{G/\rho}$ and primary wave velocity $V_p = \sqrt{(G(2-2\nu))/(\rho(1-2\nu))}$, where G is the shear modulus, and ρ and ν are the density and Poisson's ratio of the soil medium. The time of lateral shaking, $T = 2\pi/\omega$, is considered in the present analysis, where ω is the angular frequency of excitation.

A free body diagram, with the failure model considered for the present analysis, is shown in Fig. 2. For the seismic acceleration using the pseudo-dynamic method, both horizontal and vertical sinusoidal vibrations with amplitude of acceleration in the horizontal direction, a_h ($=k_h g$, where k_h is the horizontal coefficient of the seismic acceleration and g is the acceleration due to gravity), and in the vertical direction, a_v ($=k_v g$, where k_v is the vertical coefficient of the seismic acceleration), are considered. The forces acting on failure block CDFE, failure wedge ACE and failure wedge BDF are shown in Fig. 2(a), (b) and (c), respectively.

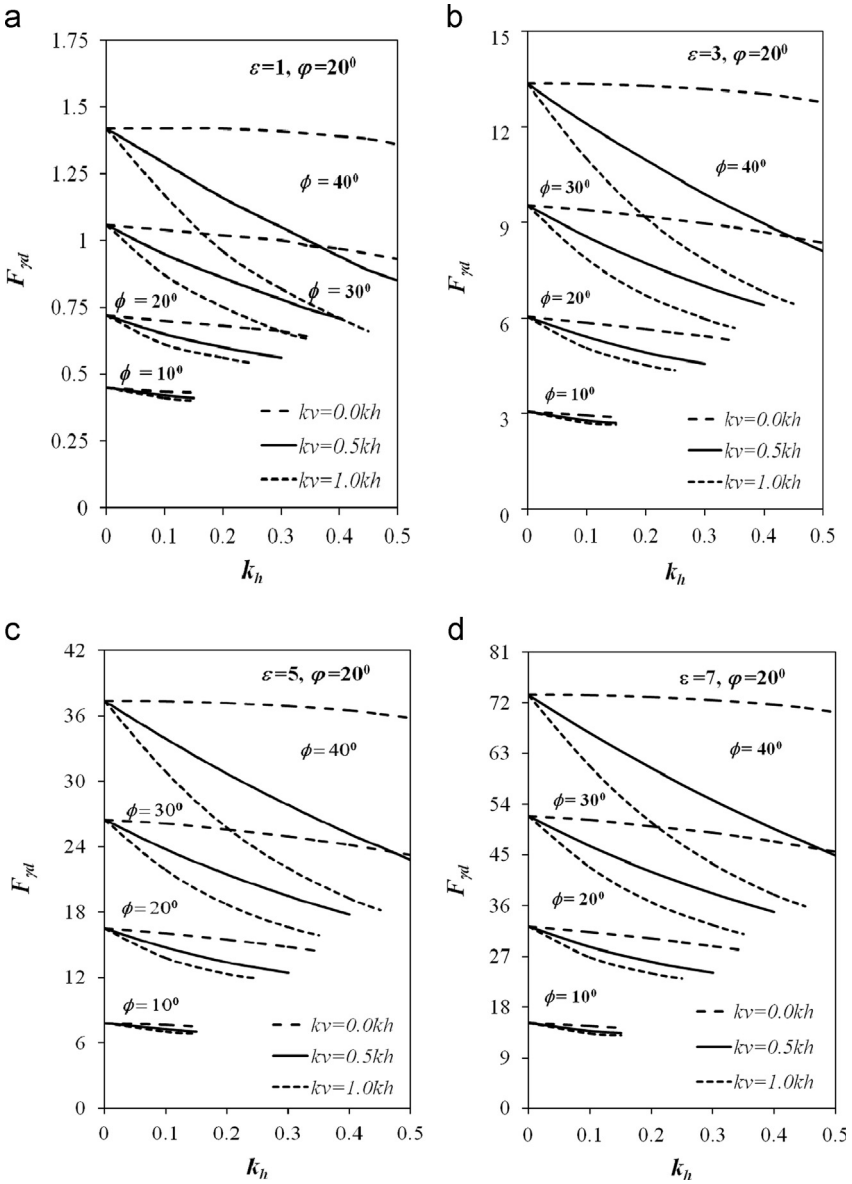

Fig. 5. Variation in $F_{\gamma d}$ for various values of k_h and k_v for $\varphi = +20^\circ$ for (a) $\varepsilon=1$, (b) $\varepsilon=3$, (c) $\varepsilon=5$ and (a) $\varepsilon=7$ with $f=1.0$, $H/\lambda=0.3$ and $H/\eta=0.16$.

Let us consider the free body diagram of wedge BDF (Fig. 2 (c)), subjected to both horizontal and vertical sinusoidal vibrations with amplitudes of acceleration a_{h1} $(=k_h g)$ and a_{v1} $(=k_v g)$, respectively. Steedman and Zeng (1990) proposed the equation of acceleration at depth z and time t acting in the horizontal direction by considering the effect of the finite shear wave velocity in terms of sinusoidal motion which was given by

$$a_h(z,t) = k_h g \ \sin\ \omega\left(t - \frac{H-z}{V_s}\right) \tag{4a}$$

Later, Nimbalkar and Choudhury (2007) modified the basic equation for seismic acceleration to consider the effect of vertical acceleration, also due to vertically propagating primary waves along with horizontal seismic acceleration, and considered the effects of time and amplification (f) in both shear and primary waves propagating though the soil. In the present study, therefore, seismic horizontal and vertical accelerations at any depth z and time t below the ground surface with soil amplification factor f can be expressed as

$$a_{h1}(z,t) = \left\{1 + \frac{H-z}{H}(f-1)\right\} a_{h1} \ \sin\ \omega\left(t - \frac{H-z}{V_s}\right) \tag{4b}$$

$$a_{v1}(z,t) = \left\{1 + \frac{H-z}{H}(f-1)\right\} a_{v1} \ \sin\ \omega\left(t - \frac{H-z}{V_p}\right) \tag{5}$$

The mass of the small incremental part of thickness dz at depth z from the ground surface in failure wedge BDF is given by

$$m_1(z) = \frac{\gamma}{g}\frac{(H-z)}{\tan\ \alpha_1}\, dz \tag{6}$$

The total weight (W_1) of failure wedge BDF is derived from Eq. (6) and yields

$$W_1 = \frac{1}{2}\frac{\gamma H^2}{\tan\ \alpha_1} \tag{7}$$

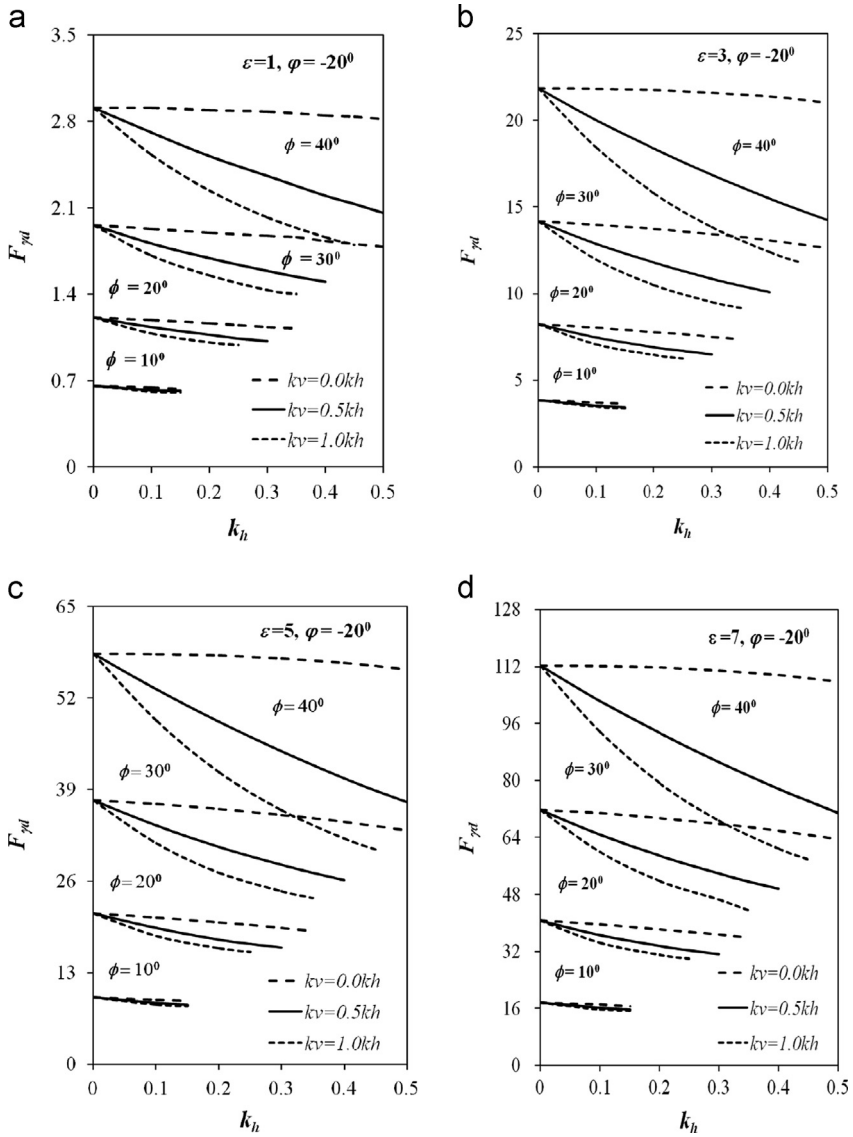

Fig. 6. Variation in $F_{\gamma d}$ for various values of k_h and k_v for $\varphi = -20^\circ$ for (a) $\varepsilon = 1$, (b) $\varepsilon = 3$, (c) $\varepsilon = 5$ and (a) $\varepsilon = 7$ with $f = 1.0$, $H/\lambda = 0.3$ and $H/\eta = 0.16$.

The horizontal seismic inertia force acting on soil wedge BDF can be written as

$$Q_{h1} = m_1(z)a_{h1}(z,t) = \int_0^H \frac{\gamma}{g}\left(\frac{H-z}{\tan\ \alpha_1}\right)\left\{1+\frac{H-z}{H}(f-1)\right\}k_h g \sin\ \omega\left(t-\frac{H-z}{V_s}\right)dz \tag{8a}$$

Integrating Eq. (8a), the total horizontal seismic inertia force can be expressed as

$$Q_{h1} = \frac{\gamma k_h}{\tan\ \alpha_1 4\pi^2}\left[2\lambda\pi H\ \cos\ \omega\zeta + \lambda^2[\ \sin\ \omega\zeta - \sin\ \omega t]\right] + \frac{\gamma k_h(f-1)}{\tan\ \alpha_1 4\pi^3}\left[2\pi^2\lambda H\ \cos\ \omega\zeta + 2\pi\lambda^2\ \sin\ \omega\zeta + \frac{\lambda^3}{H}(\cos\ \omega t - \cos\ \omega\zeta)\right] \tag{8b}$$

where $\lambda = TV_s$ is the wavelength of the vertically propagating shear wave and $\zeta = t-(H/V_s)$.

Similarly the vertical seismic inertia force acting on soil wedge BDF can be expressed as

$$Q_{v1} = m_1(z)a_{v1}(z,t) = \int_0^H \frac{\gamma}{g}\left(\frac{H-z}{\tan\alpha_1}\right)\left\{1+\frac{H-z}{H}(f-1)\right\}k_v g \sin\omega\left(t-\frac{H-z}{V_p}\right)dz \tag{9a}$$

After integrating Eq. (9a), the total vertical seismic inertia force, one can obtain

$$Q_{v1} = \frac{\gamma k_v}{\tan\ \alpha_1 4\pi^2}[2\pi\eta H\ \cos\ \omega\psi + \eta^2(\sin\ \omega\psi - \sin\ \omega t)] + \frac{\gamma k_v(f-1)}{\tan\ \alpha_1 4\pi^3}\left[2\pi^2\eta H\ \cos\ \omega\psi + 2\pi\eta^2\ \sin\ \omega\psi + \frac{\eta^3}{H}(\cos\ \omega t - \cos\ \omega\psi)\right] \tag{9b}$$

where $\eta = TV_p$ is the wavelength of the vertically propagating primary wave through the soil wedge and $\psi = t-(H/V_p)$.

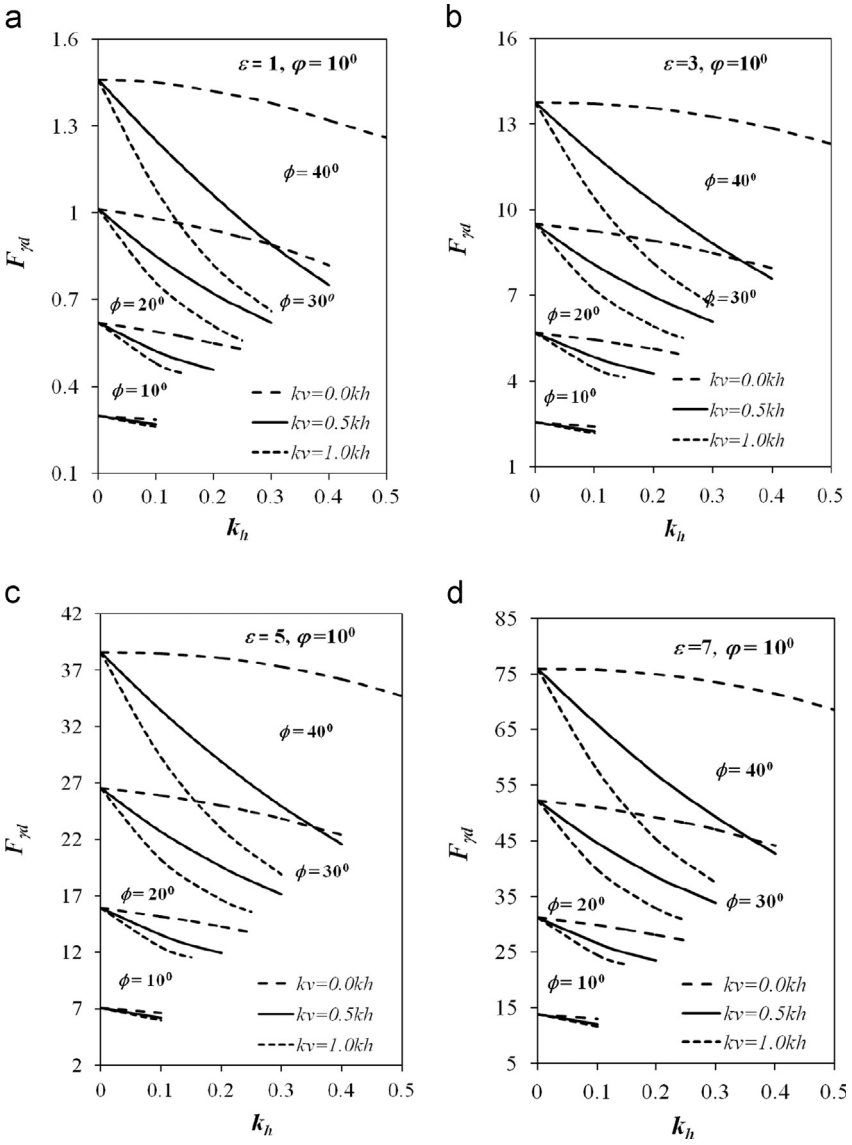

Fig. 7. Variation in $F_{\gamma d}$ for various values of k_h and k_v for $\varphi = +10^\circ$ for (a) $\varepsilon=1$, (b) $\varepsilon=3$, (c) $\varepsilon=5$ and (a) $\varepsilon=7$ with $f=1.4$, $H/\lambda=0.3$ and $H/\eta=0.16$.

Using the force equilibrium equation in horizontal and vertical directions, the seismic passive resistance ($P_{p\gamma d1}$) can be expressed as

$$P_{p\gamma d1} = [R_1 \sin(\alpha_1+\phi+\varphi) - Q_{h1} \cos\varphi - W_1 \sin\varphi + Q_{v1} \sin\varphi]/\cos(\delta+\varphi) \quad (10)$$

$$P_{p\gamma d1} = [-R_1 \cos(\alpha_1+\phi+\varphi) - Q_{h1} \sin\varphi + W_1 \cos\varphi - Q_{v1} \cos\varphi]/\sin(\delta+\varphi) \quad (11)$$

Consider the free body diagram of failure wedge ACE (Fig. 2(a)). The forces acting on wedge ACE are the W_3 weight of failure wedge ACE, and Q_{h3} and Q_{v3} are the seismic inertia force components in horizontal and vertical directions, respectively.

The horizontal seismic inertia force acting on failure wedge ACE is given by the following integral:

$$Q_{h3} = \int_0^H \frac{\gamma}{g}\left(\frac{H-z}{\tan\alpha_3}\right)\left\{1+\frac{H-z}{H}(f-1)\right\}k_h g \sin\omega\left(t-\frac{H-z}{V_s}\right)dz \quad (12a)$$

After integrating Eq. (12a), the total horizontal seismic inertia force can be expressed as

$$Q_{h3} = \frac{\gamma k_h}{\tan\alpha_3 4\pi^2}[2\lambda\pi H \cos\omega\zeta + \lambda^2(\sin\omega\zeta - \sin\omega t)] + \frac{\gamma k_h(f-1)}{\tan\alpha_3 4\pi^3}\left[2\pi^2\lambda H \cos\omega\zeta + 2\pi\lambda^2 \sin\omega\zeta + \frac{\lambda^3}{H}(\cos\omega t - \cos\omega\zeta)\right] \quad (12b)$$

Similarly, the vertical seismic inertia force is given by the integral

$$Q_{v3} = \int_0^H \frac{\gamma}{g}\left(\frac{H-z}{\tan\alpha_3}\right)\left\{1+\frac{H-z}{H}(f-1)\right\}k_v g \sin\omega\left(t-\frac{H-z}{V_p}\right)dz \quad (13a)$$

The total vertical seismic inertia force can be obtained by integrating Eq. (13a) as

$$Q_{v3} = \frac{\gamma k_v}{\tan\alpha_3 4\pi^2}[2\pi\eta H \cos\omega\psi + \eta^2(\sin\omega\psi - \sin\omega t)]$$

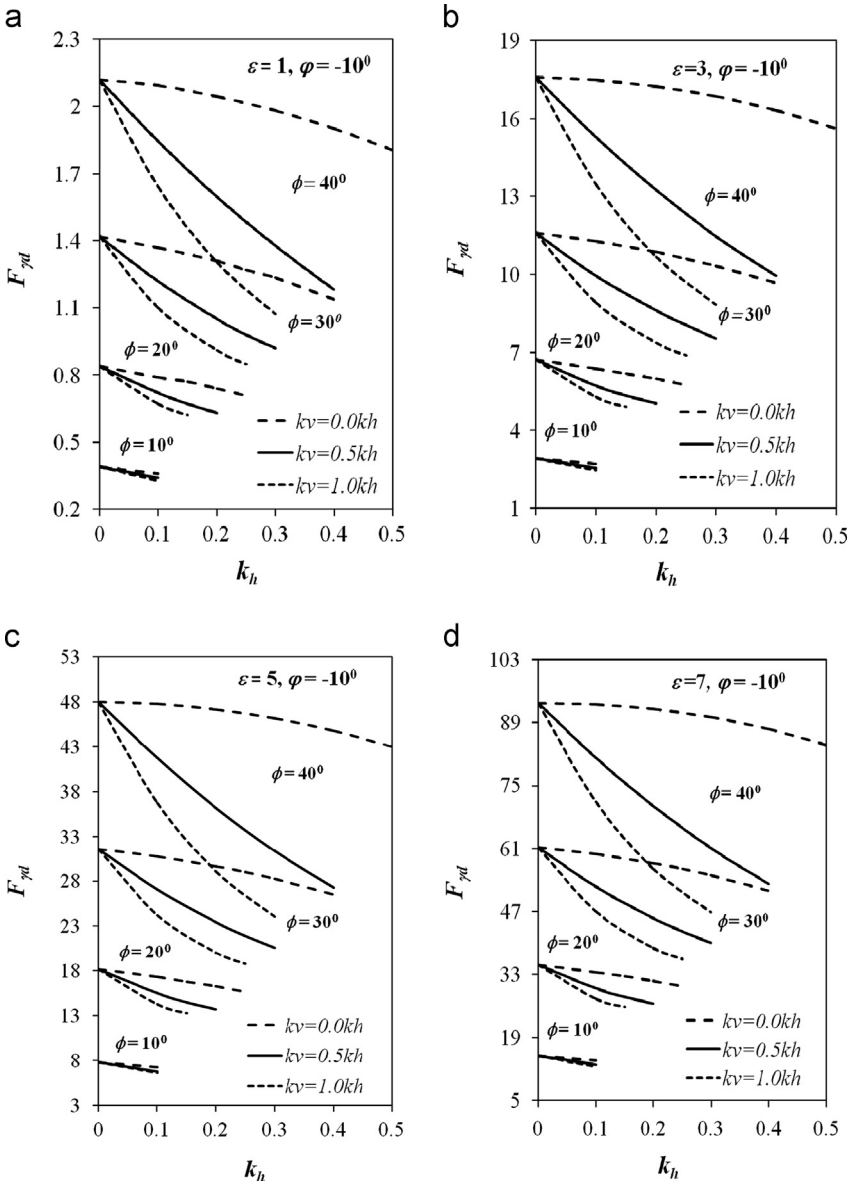

Fig. 8. Variation in $F_{\gamma d}$ for various values of k_h and k_v for $\varphi = -10^\circ$ for (a) $\varepsilon=1$, (b) $\varepsilon=3$, (c) $\varepsilon=5$ and (a) $\varepsilon=7$ with $f=1.4$, $H/\lambda=0.3$ and $H/\eta=0.16$.

$$+\frac{\gamma k_v(f-1)}{\tan\ \alpha_3 4\pi^3}\left[2\pi^2\eta H\ \cos\ \omega\psi+2\pi\eta^2\ \sin\ \omega\psi+\frac{\eta^3}{H}(\cos\ \omega t-\ \cos\ \omega\psi)\right] \quad (13b)$$

The seismic passive resistance ($P_{P\gamma d3}$) acting on face CE can be obtained from the force equilibrium equation in horizontal and vertical directions as

$$P_{p\gamma d3}=[R_3\ \sin(\alpha_3+\phi-\varphi)+W_3\ \sin\ \varphi+Q_{h3}\ \cos\ \varphi-Q_{v3}\ \sin\ \varphi]/\ \cos(\delta-\varphi) \quad (14)$$

$$P_{p\gamma d3}=[-R_3\ \cos(\alpha_3+\phi-\varphi)+W_3\ \cos\ \varphi-Q_{h3}\times\sin\ \varphi-Q_{v3}\ \cos\ \varphi]/\ \sin(\delta-\varphi) \quad (15)$$

Consider the elementary strip of thickness dz at depth z from the ground surface in rectangular failure block CDFE (Fig. 2(b)). The mass of the elementary strip is given by

$$m_2(z)=\frac{\gamma\ Bdz}{g} \quad (16)$$

The total weight of failure block CDFE, W_2, is obtained from Eq. (16), namely,

$$W_2=\gamma\ BH \quad (17)$$

The total horizontal seismic inertia force acting on soil block CDFE can be obtained as

$$Q_{h2}=\int_0^H\frac{\gamma Bdz}{g}\left\{1+\frac{H-z}{H}(f-1)\right\}k_h g\ \sin\ \omega\left(t-\frac{H-z}{V_s}\right)=\frac{\gamma Bk_h}{4\pi^2}\left[2\pi\lambda(\cos\ \omega\zeta-\ \cos\ \omega t)+2\pi\lambda(f-1)\times\ \cos\ \omega\zeta+\frac{\lambda^2(f-1)(\sin\ \omega\zeta-\ \sin\ \omega t)}{H}\right] \quad (18)$$

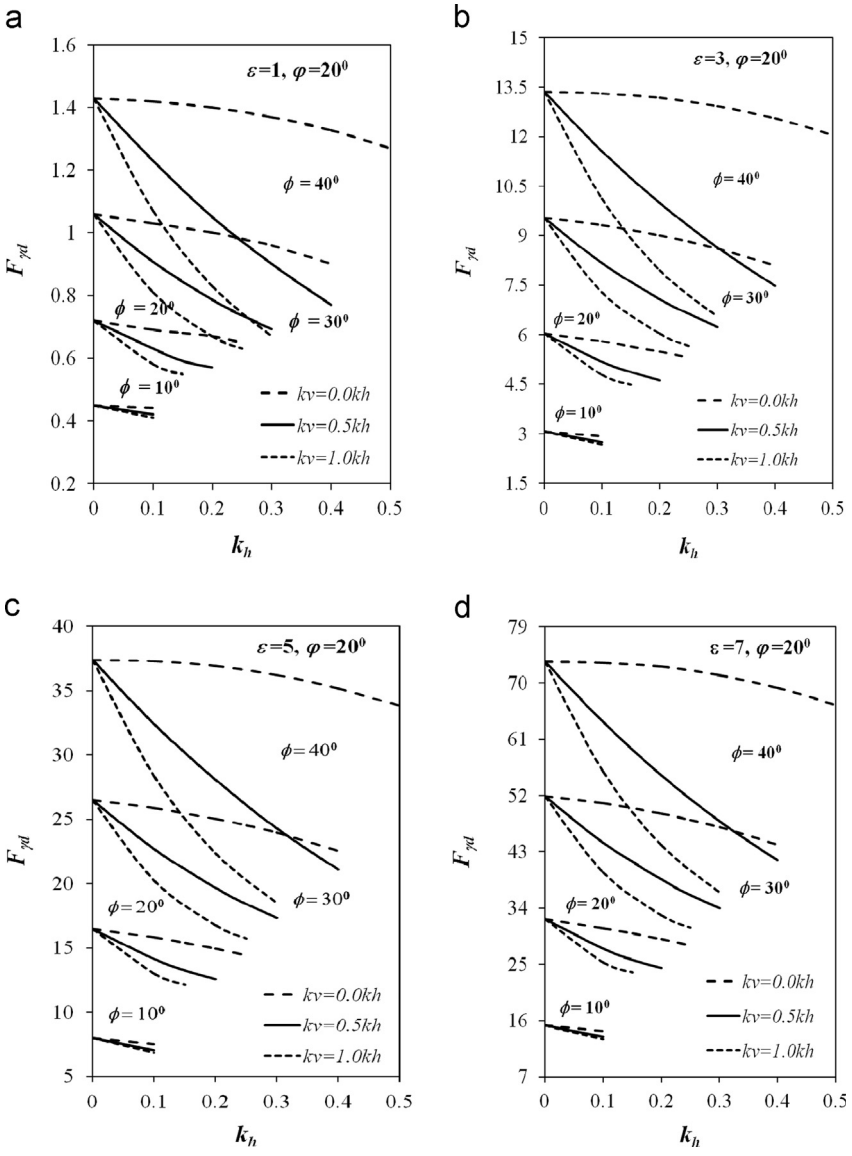

Fig. 9. Variation in $F_{\gamma d}$ for various values of k_h and k_v for $\varphi=+20^\circ$ for (a) $\varepsilon=1$, (b) $\varepsilon=3$, (c) $\varepsilon=5$ and (a) $\varepsilon=7$ with $f=1.4$, $H/\lambda=0.3$ and $H/\eta=0.16$.

The total vertical seismic inertia force acting on soil block CDEF can be given by

$$Q_{v2} = \int_0^H \frac{\gamma B dz}{g}\left\{1+\frac{H-z}{H}(f-1)\right\}k_v g \sin\omega\left(t-\frac{H-z}{V_p}\right)$$
$$= \frac{\gamma B k_v}{4\pi^2}\left[2\pi\eta(\cos\omega\psi-\cos\omega t)+2\pi\eta(f-1)\cos\omega\psi + \frac{\eta^2(f-1)(\sin\omega\psi-\sin\omega t)}{H}\right] \quad (19)$$

The seismic passive resistance acting on the imaginary faces of retaining walls (Choudhury and Subba Rao, 2004), DF and CE, are $P_{p\gamma d1}$ and $P_{p\gamma d3}$, respectively. As mentioned by Meyerhof and Adams (1968), the anchor uplift capacity is an application of the retaining wall problem under the negative wall friction angle case of passive earth pressure under the static condition due to the movement of the anchor block. Similar consideration was given by Choudhury and Subba Rao (2004) for the pseudo-static seismic analysis and applied in the present pseudo-dynamic analysis for imaginary wall movement.

The gross seismic pullout load (P_{ud}) of an anchor is given by

$$P_{ud} = P_{p\gamma d1}\ \sin(\delta+\varphi)+P_{p\gamma d3}\ \sin(\delta-\varphi) + W_2\ \cos\ \varphi-Q_{v2}\ \cos\ \varphi-Q_{h2}\ \sin\ \varphi \quad (20)$$

The net ultimate seismic uplift capacity of anchor q_{udnet} is given by

$$q_{udnet} = \frac{P_{ud}-[W_2\ \cos\ \varphi-Q_{v2}\ \cos\ \varphi-Q_{h2}\ \sin\ \varphi]}{B} \quad (21)$$

On simplification, q_{udnet} can be written in the following form:

$$q_{udnet} = 0.5\gamma B F_{\gamma d} \quad (22)$$

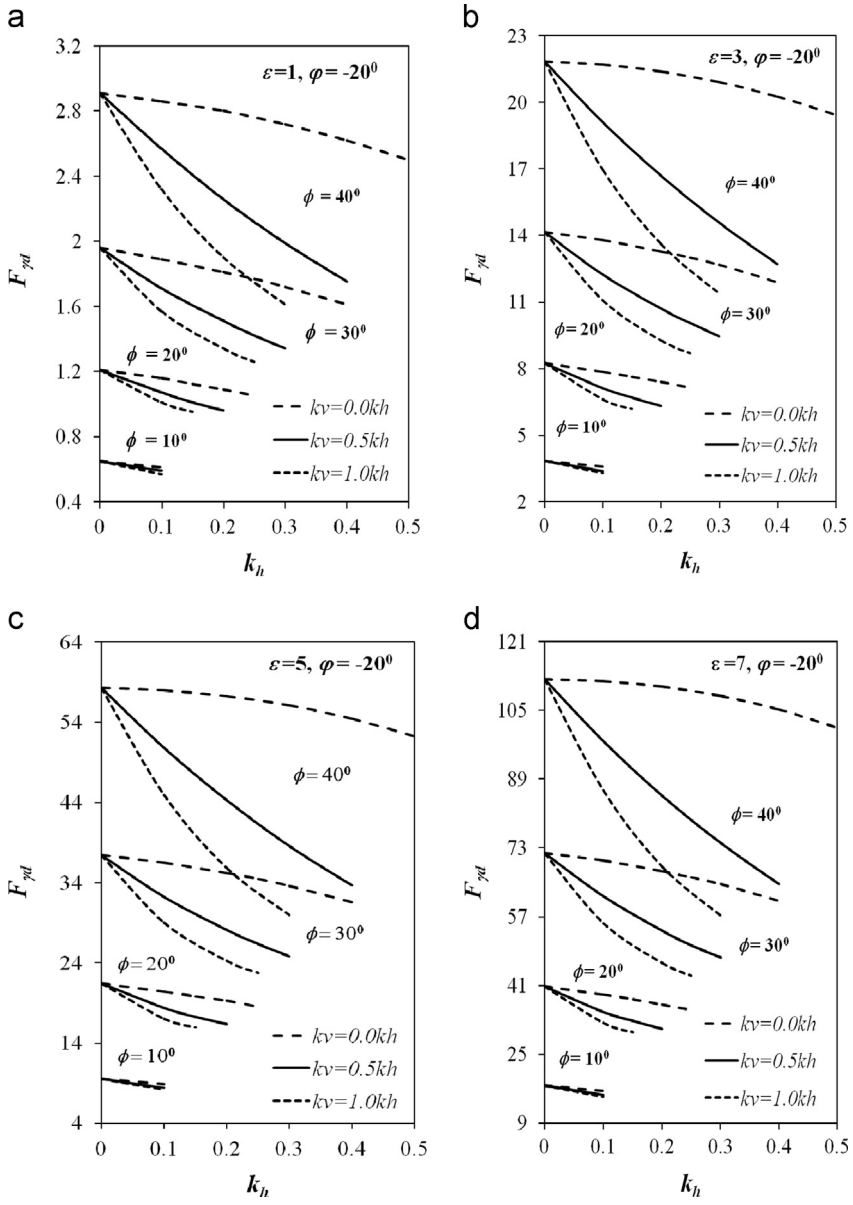

Fig. 10. Variation in $F_{\gamma d}$ for various values of k_h and k_v for $\varphi=-20^\circ$ for (a) $\varepsilon=1$, (b) $\varepsilon=3$, (c) $\varepsilon=5$ and (a) $\varepsilon=7$ with $f=1.4$, $H/\lambda=0.3$ and $H/\eta=0.16$.

The net seismic uplift capacity factor in the above expression ($F_{\gamma d}$) can be given as

$$F_{\gamma d} = \varepsilon^2 K_{p\gamma d}[\tan(\delta+\varphi)+\tan(\delta-\varphi)]-2\varepsilon \sin\varphi \tan(\delta-\varphi) + \frac{k_v \sin\varphi}{2\pi^2 B}\left[2\pi\eta(\cos\omega\psi-\cos\omega t)+2\pi\eta(f-1)\cos\omega\psi + \frac{\eta^2(f-1)(\sin\omega\psi-\sin\omega t)}{H}\right]\tan(\delta-\varphi) - \frac{k_h \cos\varphi}{2\pi^2 B}\left[2\pi\lambda(\cos\omega\zeta-\cos\omega t)+2\pi\lambda(f-1) \times \cos\omega\zeta + \frac{\lambda^2(f-1)(\sin\omega\zeta-\sin\omega t)}{H}\right]\tan(\delta-\varphi) \quad (23)$$

where $K_{p\gamma d}$ is the net seismic passive earth pressure coefficient for the unit weight component and the embedment ratio of the anchor, $\varepsilon = H/B$.

The net seismic uplift capacity factor ($F_{\gamma d}$) can be obtained from the above expression for different combinations of load inclination, soil friction angle, seismic acceleration coefficients in both vertical and horizontal directions, soil amplification factor and embedment ratio of a shallow horizontal plate anchor subjected to an oblique load.

In the present analysis, the value of $V_p/V_s = 1.87$ is considered by using the relationship between the primary and the shear wave velocities with Poison's ratio of the soil (Das, 1993). It can be observed from Eq. (23) that $F_{\gamma d}$ is a function of the angle of the failure plane, t/T, H/λ and H/η. The minimum value for $F_{\gamma d}$ is obtained by optimizing $F_{\gamma d}$ with respect to the angle of the failure planes and t/T.

2.1. Determination of critical angle of failure plane

The critical angle of failure planes depends on the soil friction angle and remains constant under static conditions, whereas under seismic conditions, it shifts with changes in the input parameters, like k_h, k_h and soil amplification in addition to ϕ. Hence, a trial and error procedure is used in the present analysis to find the critical angle of the failure planes for different combinations of seismic acceleration coefficients in both horizontal and vertical directions with the amplification factor and the inclination of load for various values of the soil friction angle. The trial values obtained for α_1 and α_3 must satisfy the condition whereby the two computed values for $P_{p\gamma d1}$, from Eqs. (10) and (11), and $P_{p\gamma d3}$, from Eqs. (14) and (15), are the same. The critical values for α_1 and α_3 are obtained until a convergence is reached to the third decimal for various values of ϕ with different combinations of k_h, k_v, φ and f.

3. Results and discussion

The equation proposed in the case of cohesionless soil to avoid the phenomenon of shear fluidization for various combinations of k_h and k_v (Richards et al., 1990) and modified by Ghosh (2009) for the amplification effect, f, for the values of ϕ, is considered and given by

$$\phi \geq \tan^{-1}\left[\frac{fk_h}{1-fk_v}\right] \quad (24)$$

The results for $F_{\gamma d}$ for a horizontal strip anchor subjected to an oblique load are presented in a combination of graphs and tables. The different input parameters, such as ϕ, φ, k_h, k_v, ε, f and their variations, are considered in the present study.

Figs. 3 and 4 show the variations in $F_{\gamma d}$ with k_h for various combinations of k_v and different values for ϕ, ε with f =1.0, H/λ=0.3 and H/η=0.16 for φ=+10° and φ=−10°, respectively. Similarly, Figs. 5 and 6 show the variations in $F_{\gamma d}$ with k_h for

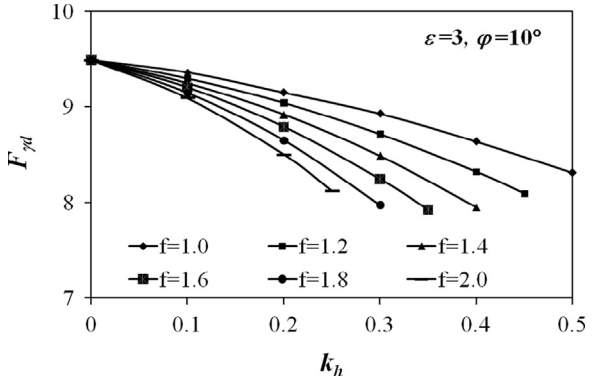

Fig. 11. Effect of soil amplification factor on $F_{\gamma d}$ for different values of k_h with k_v=0.0k_h for ϕ=30^0, φ=+10°, ε=3.0, H/λ=0.3 and H/η=0.16.

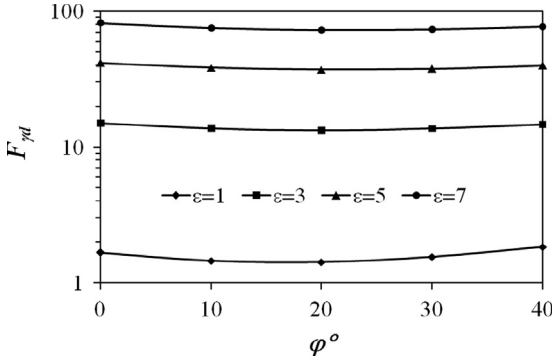

Fig. 12. Variation in $F_{\gamma d}$ for various positive values of φ for k_h=0.2, k_v=0.0k_h for ϕ=40^0 with f =1.0, H/λ=0.3 and H/η=0.16.

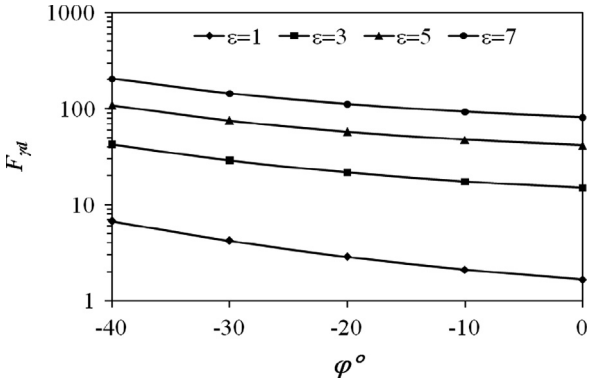

Fig. 13. Variation in $F_{\gamma d}$ for various negative values of φ for k_h=0.2, k_v=0.0k_h for ϕ=40^0, with f=1.0, H/λ=0.3 and H/η=0.16.

various combinations of k_v, and different values for ϕ, ε with f=1.0, H/λ=0.3 and H/η=0.16 for $\varphi=+20^\circ$ and $\varphi=-20^\circ$, respectively. Again, Figs. 7 and 8 are drawn for $\varphi=\pm 10^\circ$, respectively, whereas Figs. 9 and 10 are plotted for $\varphi=\pm 20^\circ$, respectively, to show the variations in $F_{\gamma d}$ with k_h for various combinations of k_v, and different values for ϕ, ε with f=1.4, H/λ=0.3 and H/η=0.16. Fig. 11 shows the effect of the amplification factor on $F_{\gamma d}$ for different values of k_h with $k_v=0.0k_h$ for $\phi=30^\circ$, $\varphi=10^\circ$, $\varepsilon=3.0$, $H/\lambda=0.3$ and $H/\eta=0.16$.

It can be observed that $F_{\gamma d}$ marginally decreases with an increase in the inclination of the anchor load up to $+20^\circ$, and thereafter, $F_{\gamma d}$ increases with an increase in φ (Fig. 12). A significant increase in $F_{\gamma d}$ values with an increase in the negative inclination of the load is observed (Fig. 13). The values for $F_{\gamma d}$ decrease with an increase in the amplification factor and the inclination of the load in either direction for all the combinations of seismic acceleration coefficients in both horizontal and vertical directions. For example, referring to Fig. 3, Fig. 4 and Table 1, for the case of $\phi=30^0$, $k_h=0.1$, $k_v=0.0k_h$, $\varepsilon=5$ and $f=1.4$, it is observed that the net seismic uplift capacity factor decreases by 5.86% for $\varphi=+10^\circ$ and increases by 10.76% for $\varphi=-10^\circ$ if compared with the values for $F_{\gamma d}$ for $\varphi=0^\circ$ and the difference increases with an increase in k_v and φ in both directions of load inclination. Again, from Figs. 5 and 9, for the case of $\phi=40^\circ$, $\varepsilon=5$, $k_h=0.2$ and $k_v=0.5k_h$, it is seen that the value for $F_{\gamma d}$ with f=1.0 is 1.09 times more than the value with f=1.4 for $\varphi=+20^\circ$.

It is observed that the inclinations of failure planes AC and BD keep changing with changes in the soil friction angle, both seismic acceleration coefficients in horizontal and vertical directions and the amplification factor. From Table 2, it is seen that α_3 increases and α_1 decreases with an increase in k_h in the critical direction, as shown in Fig. 1. Similarly, both α_3 and α_1 increase significantly with an increase in the seismic acceleration coefficient in the vertical direction. Referring to Table 3, for $\varphi=30^\circ$ and $\phi=40^\circ$, $k_h=0.1$ and $f=1.0$, α_1 and α_3

Table 1
Values of $F_{\gamma d}$ for variation in φ for various values of k_v and ϕ with $k_h=0.1$, $\varepsilon=5$, $f=1.4$, $H/\lambda=0.3$ and $H/\eta=0.16$.

ϕ	k_v	$\varphi=-40^\circ$	$\varphi=-30^\circ$	$\varphi=-20^\circ$	$\varphi=-10^\circ$	$\varphi=0^\circ$	$\varphi=10^\circ$	$\varphi=20^\circ$	$\varphi=30^\circ$	$\varphi=40^\circ$
30°	$0.0k_h$	62.61	45.99	36.48	30.76	27.45	25.93	25.87	27.19	29.93
	$0.5k_h$	55.98	40.89	32.24	27.04	24.05	22.68	22.67	23.91	26.47
	$1.0k_h$	50.98	36.99	29.01	24.21	21.46	20.22	20.23	21.42	23.84
40°	$0.0k_h$	109.02	75.43	57.95	59.79	41.77	38.48	37.26	37.79	40.02
	$0.5k_h$	96.49	66.47	50.82	52.52	36.36	33.44	32.39	32.94	35.02
	$1.0k_h$	86.13	59.06	44.93	46.98	31.88	29.28	28.37	28.93	30.88

Table 2
Values for inclination of failure planes for various values of k_h with $k_v=0.0k_h$, $\varepsilon=1$, $\phi=30^\circ$, $\varphi=10^\circ$, $f=1.0$, $H/\lambda=0.3$ and $H/\eta=0.16$.

k_h	0.0	0.1	0.2	0.3	0.4	0.5
$\alpha_1^{(\circ)}$	52.9	51.18	49.48	47.81	46.16	44.57
$\alpha_3^{(\circ)}$	52.9	54.61	56.3	58.01	59.65	61.27

Table 3
Values for inclination of failure planes for various values of ϕ and f for $k_h=0.1$, $\varepsilon=3$, $\varphi=30^\circ$, $H/\lambda=0.3$ and $H/\eta=0.16$.

ϕ	k_v/k_h	f=1.0		f=1.4	
		$\alpha_1^{(\circ)}$	$\alpha_3^{(\circ)}$	$\alpha_1^{(\circ)}$	$\alpha_3^{(\circ)}$
10°	0.0	56.03	59.01	55.30	59.69
	0.5	67.31	69.60	70.55	73.29
	1.0	74.82	75.89	78.4	79.48
20°	0.0	53.55	56.80	52.85	57.51
	0.5	59.91	62.92	61.9	65.90
	1.0	65.62	68.05	69.34	72.14
30°	0.0	51.18	54.61	50.46	55.35
	0.5	55.60	59.01	56.85	61.49
	1.0	59.87	62.98	62.88	66.88
40°	0.0	48.90	52.51	48.15	53.28
	0.5	52.25	55.90	53	58.15
	1.0	55.65	59.18	57.91	62.80

are 48.90 and 52.51 for $k_h=0.0k_h$ increases to 52.25 and 55.90, respectively, for $k_h=0.5k_h$. The inclination of the failure planes further increases in the presence of the soil amplification factor resulting in the formation of steeper failure planes. It is worth noting that the embedment ratio does not affect the geometry of the failure planes even under seismic conditions, which shows a resemblance to the observation under static conditions, whereas the reverse observation was proposed by Ghosh (2009). From Table 2, for $\phi=30^\circ$ and $\varphi=10^\circ$, $k_h=0.1$, $k_v=0.0$, $f=1.0$ and from Table 3 for $\phi=30^\circ$, $\varphi=30^\circ$, $k_h=0.1$, $k_v=0.0$, $f=1.0$ values of α_1 and α_3 are the same, i.e., 51.18 and 54.61, respectively. It is also observed from Tables 2 and 3 that the anchor inclination does not change the geometry of the failure planes, which shows a resemblance to the prediction by Das and Seeley (1975).

Fig. 11 shows the effect of the amplification factor on the values for the net uplift capacity factor for $\phi=30^\circ$ with $\varphi=+10^\circ$, $\varepsilon=3.0$, $H/\lambda=0.3$ and $H/\eta=0.16$ for different values of k_h with $k_v=0.0k_h$. It shows that $F_{\gamma d}$ decreases continuously with an increase in the soil amplification factor and the seismic acceleration coefficient in the horizontal direction. Referring to Fig. 11, $F_{\gamma d}$ decreases by 1.22% if the amplification factor (f) changes from 1 to 1.2, 1.35% for a change in f from 1.2 to 1.4, 1.47% for a change in f from 1.4 to 1.6, 1.62% when f changes from 1.6 to 1.8, 1.65% for a change in f from 1.8 to 2.0. From Figs. 4–10, it is also observed that $F_{\gamma d}$ decreases with an increase in k_v and f for all possible inclinations of load. Hence, proper attention must be given by a geotechnical engineer to determine the effect of soil amplification on $F_{\gamma d}$ as it may lead to the catastrophic failure of anchors under seismic conditions. Previously, very few researchers obtained the uplift capacity for an oblique loaded anchor under static conditions. The present study shows the importance of obtaining the uplift capacity under seismic conditions considering the effect of amplification.

4. Comparison of results

Table 4 shows a comparison of the breakout factor ($q_{ud}=P_{ud}/A\gamma H$) in medium–dense sand under static conditions ($k_h=k_v=0.0$) for the test data of Das and Seeley (1975) with $B=0.064$ m and $\gamma=14.71$ kN/m^3, $\phi=31^\circ$. The shape factors proposed by Tagaya et al. (1988) are used for the comparison. Up to an embedment ratio of 2, the proposed theory follows the experimental results closely; thereafter, for $\varepsilon=4.5$ it over predicts the results (by 15.21%). The shape factors used for the comparison are lower than the values recommended by Meyerhof and Adams (1968) and higher than those recommended by Dickin and Laman (2007).

The results of the present study and the test results obtained by Meyerhof (1973) for $\phi=43^\circ$ for a gross pullout load of a horizontal strip anchor subjected to an inclined load are given in Table 5. The results obtained in the present study are in favorable comparison with the experimental results and follow a similar trend, showing a constant decrease in the gross pullout load, except the marginal shift when φ changes from 30° to 40°. In the present study, the gross pullout load increases by 2.21% and decreases by 0.49% for Meyerhof (1973), when φ changes from 30° to 40°.

The experimental results of Dickin and Laman (2007), for loose sand with $B=1$ m, $\gamma=14.5$ kN/m^3, $\phi=35^\circ$ under static conditions, are compared with the predictions of theoretical

Table 5
Comparison of gross pullout capacity, P_{ud}(N/m), with experimental results by Meyerhof (1973) under static condition ($k_h=k_v=0.0$).

φ	Present study	Meyerhof (1973)
0°	202	228
10°	187	2160
20°	179	208
30°	177	205
40°	181	204

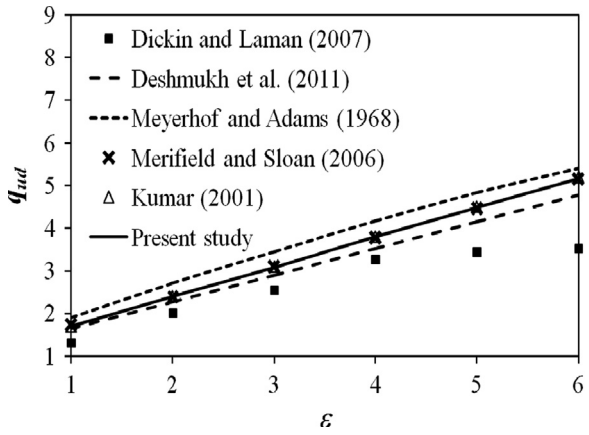

Fig. 14. Comparison of breakout factor (q_{ud}) with experimental results of Dickin and Laman (2007) with $\gamma=14.5$ kN/m^3, $B=1$ m and $\phi=35^\circ$ under static conditions ($k_h=k_v=0.0$).

Table 4
Comparison of breakout factor (q_{ud}) with experimental results by Das and Seeley (1975) under static condition ($k_h=k_v=0.0$).

φ	Das and Seeley (1975)			Present study		
	$\varepsilon=1$	$\varepsilon=2$	$\varepsilon=4.5$	$\varepsilon=1$	$\varepsilon=2$	$\varepsilon=4.5$
0°	1.53	2.08	3.29	1.58	2.17	3.65
10°	1.79	2.99	3.91	1.73	2.37	3.97
20°	2.44	3.92	4.37	1.96	2.68	4.5
30°	2.768	4.49	4.57	2.34	3.21	5.39
40°	3.23	4.84	4.86	3.06	4.16	6.97

methods, as shown in Fig. 14. The solutions obtained by Deshmukh et al. (2011) and Kumar (2001), the lower bound results by Merifield and Sloan (2006) and the proposed method show a favorable agreement with the experimental results up to $\varepsilon=4.0$; thereafter, they overpredict. The theory of Meyerhof and Adams (1968) overestimates the uplift capacity with the observed one. For a horizontal strip anchor subjected to vertical load under static conditions, Merifield and Sloan (2006) quantify the effect of anchor roughness, which is less than 4%, and hence, justifies the assumption of the smooth plate in the present study.

Table 6 shows a comparison of q_{ud} with the available results in literature under seismic conditions for $\phi=30^\circ$, $\varphi=0^\circ$, $f=1.0$, $\varepsilon=1$, $H/\lambda=0.3$ and $H/\eta=0.16$. It is observed that the present study shows a reasonable comparison with the results obtained by other researchers (Choudhury and Subba Rao, 2004; Kumar, 2001; Ghosh, 2009) for $\varepsilon=1$ with various combinations for k_h and k_v. The difference in the results obtained in the present study and those by Choudhury and Subba Rao (2004) is found to vary about 1.28% to −5%, −4.16% to 1% with Kumar (2001).

The ultimate seismic uplift capacity factor, $F_{\gamma E}$ $(=P_{ud}/\gamma B^2)$, using the upper bound solution, was obtained by Ghosh (2009) for a horizontal strip anchor using the pseudo-dynamic approach. Table 7 shows a comparison of $F_{\gamma E}$, for which various values for k_h and k_v are considered for $\phi=30^\circ$, $\varphi=0^\circ$, $\varepsilon=5$, $f=1.0$ and 1.4, $H/\lambda=0.3$ and $H/\eta=0.16$. It is observed that the present study predicts lower values than Ghosh (2009) for the given combinations of k_h and k_v with various amplification factors. The percentage difference of the present theory, observed for $f=1.0$ ranges between −1.78% and −5.27% for $k_v=0.0k_h$; −1.78% to −6.15% for $k_v=0.5k_h$ for different values of k_h and difference increases with an increase in f (=1.4), with Ghosh (2009). This difference in results can be attributed to the inherent differences between the limit analysis method and the limit equilibrium method, thus showing the adequacy of the present theory.

5. Conclusions

The net seismic uplift capacity factor for an obliquely loaded horizontal strip anchor for the unit weight component of soil ($F_{\gamma d}$) is computed using the limit equilibrium method with a pseudo-dynamic approach. Kötter (1903) is employed to obtain the distribution of soil reaction on a simple planar failure surface. It is observed that $F_{\gamma d}$ decreases for a certain positive inclination of load ($\varphi \cong +20^\circ$); thereafter, it increases and a significant increase in the results was observed for the inclination of load in a negative direction under seismic conditions. $F_{\gamma d}$ decreases significantly with an increase in the seismic acceleration coefficients in both vertical and horizontal directions and the amplification factor and increases with an increase in the embedment ratio and the soil friction angle, as expected. The values obtained from the present analysis are compared with the available specific results reported in literature under both static and seismic conditions and are found to be in good agreement with them. Hence, Kötter (1903) worked as a powerful tool in the present analysis, namely, to obtain the uplift capacity factor which shows the better agreement with the results available in literature, obtained by the pseudo-static, pseudo-dynamic approach, using various approaches like the complicated upper bound limit method, the log-spiral failure surface and even the experimental results.

Table 6
Comparison of q_{ud} for $\phi=30^\circ$, $\varphi=0^\circ$, $f=1.0$, $\varepsilon=1$, $H/\lambda=0.3$ and $H/\eta=0.16$.

k_h	Present study		Choudhury and Subba Rao (2004)		Kumar (2001)	
	$k_v=0.5k_h$	$k_v=1.0k_h$	$k_v=0.5k_h$	$k_v=1.0k_h$	$k_v=0.5k_h$	$k_v=1.0k_h$
0	1.56	1.56	1.54	1.54	1.58	1.58
0.1	1.44	1.37	1.45	1.37	1.49	1.40
0.2	1.32	1.18	1.35	1.20	1.38	1.22
0.3	1.20	1.00	1.26	1.03	1.25	0.99

Table 7
Comparison of $F_{\gamma E}$ for $f=1.0$ and 1.4, $\phi=30^\circ$, $\varphi=0^\circ$, $\varepsilon=5$, $H/\lambda=0.3$ and $H/\eta=0.16$.

k_h	Ghosh (2009)				Present study			
	$f=1.0$		$f=1.4$		$f=1.0$		$f=1.4$	
	$k_v=0.0k_h$	$k_v=0.5k_h$	$k_v=0.0k_h$	$k_v=0.5k_h$	$k_v=0.0k_h$	$k_v=0.5k_h$	$k_v=0.0k_h$	$k_v=0.5k_h$
0.0	19.43	19.43	19.43	19.43	19.09	19.09	19.09	19.09
0.1	19.41	18.51	19.38	18.22	18.87	17.64	18.73	16.93
0.2	19.28	17.42	19.24	16.91	18.60	16.41	18.24	15.19
0.3	19.09	16.28	18.87	15.45	18.26	15.34	17.61	13.81
0.4	18.79	15.08	18.36	–	17.85	14.46	16.82	–

Note: '–' shows the case of shear fluidization (Richards et al., 1990; Ghosh, 2009).

Nomenclature

a_h	amplitude of acceleration in the horizontal direction
a_v	amplitude of acceleration in the vertical direction
B	width of ground anchor
dp	differential reaction pressure on failure surface
f	amplification factor
$F_{\gamma d}$	net seismic uplift capacity factor
$F_{\gamma E}$	ultimate seismic uplift capacity factor
H	depth of anchor from ground
G	shear modulus
k_h	seismic coefficient of acceleration in the horizontal direction
k_v	seismic coefficient of acceleration in the vertical direction
L	length of anchor
P_{ud}	gross seismic pullout capacity
$P_{p\gamma d1}$, $P_{p\gamma d3}$	seismic passive resistance acting on an imaginary faces of retaining wall
q_{ud}	breakout factor
Q_h	total horizontal inertia force
Q_v	total vertical inertia force
$R_{1,3}$	resultant soil reaction on failure planes
S	length of failure plane
t	time
T	period of lateral shaking
V_p	primary wave velocity
V_s	shear wave velocity
W	total weight of failure wedge
W_1, W_2 and W_3	weights of respective failure wedges
z	depth of point below ground level
ϕ	soil friction angle
δ	wall friction angle
α	inclination of tangent on failure surface at the point of interest with horizontal
α_1, α_3	angles of failure planes with horizontal
ε	embedment ratio
γ	unit weight of soil
ω	angular frequency
ρ	density of soil medium
ν	Poisson's ratio of soil medium
λ	wavelength of the vertically propagating shear wave
η	wavelength of the vertically propagating primary wave
φ	angle of pullout load with vertical.

References

Balla, A., 1961. The resistance to breaking out of mushroom foundations for pylons. In: Proceedings of the Fifth International Conference on Soil Mechanics and Foundation Engineering, vol. I, Paris, France, pp. 569–576.

Chattopadhayay, B.C., Pise, P.J., 1986. Breakout resistance of horizontal anchors in sand. Soils and Foundations 26 (4), 16–22.

Choudhury, D., Nimbalkar, S., 2005. Seismic passive resistance by pseudo dynamic method. Geotechnique 55 (9), 699–702.

Choudhury, D., Subba Rao, K.S., 2005a. Seismic uplift capacity of inclined strip anchors. Canadian Geotechnical Journal 42 (1), 263–271.

Choudhury, D., Subba Rao, K.S., 2005b. Seismic bearing capacity of shallow strip footings. Geotechnical and Geological Engineering 23 (4), 403–418.

Choudhury, D., Subba Rao, K.S., 2004. Seismic uplift capacity of strip anchors in soil. Geotechnical and Geological Engineering 22 (1), 59–72.

Choudhury, D., Subba Rao, K.S., 2002. Seismic passive resistance in soils for negative wall friction. Canadian Geotechnical Journal 39 (4), 971–981.

Das, B.M., 1993. Principals of Soil Dynamics. PWS-KENT Publishing Company, Boston, MA (Boston, Massachusetts).

Das, B.M., Seeley, G.R., 1975. Inclined load resistance of anchors in sand. Proceedings of the American Society of Civil Engineers 2 (GT 9), 995–1003.

Deshmukh, V.B., Dewaikar, D.M., Choudhary, D., 2011. Uplift capacity of horizontal strip anchors in cohesionless soil. Geotechnical and Geological Engineering, vol. 29. Springer, Netherlands977–988.

Dickin, E.A., Laman, M., 2007. Uplift response of the strip anchor in cohesionless soil. Advances in Engineering Software 38 (8–9), 618–625.

Ghosh, P., 2009. Seismic vertical uplift capacity of horizontal strip anchors using pseudo-dynamic approach. Computers and Geotechnics 36 (1–2), 342–351.

Honda, T., Hirai, Y., Sato, E., 2011. Uplift capacity of belled and multi-belled piles in dense sand. Soils and Foundations 51 (3), 483–496.

Hugo, E.A.-M., Gourvenec, S.M., Randolph, M.F., 2010. Effect of gapping on the transient and sustained uplift capacity of a shallow skirted foundation in clay. Soils and Foundations 50 (5), 725–735.

Kötter, F., 1903. Die Bestimmung des Drucks an gekrümmten Gleitflächen, eine Aufgabe aus der Lehre vom Erddruck. Sitzungsberichte der Akademie der Wissenschaften Berlin, 229–233.

Kumar, J., Kouzer, K.M., 2008. Vertical uplift capacity of horizontal anchors using upper bound limit analysis and finite elements. Canadian Geotechnical Journal 45 (5), 698–704.

Kumar, J., 2001. Seismic vertical uplift capacity of strip anchors. Geotechnique 51 (3), 275–279.

Kumar, J., 1999. Kinematic slices approach for uplift analysis of strip anchors. International Journal for Numerical and Analytical Methods in Geomechanics 23 (11), 1159–1170.

Matsuo, M., 1967. Study on uplift resistance of footing (I). Soils and Foundations 7 (4), 1–37.

Matsuo, M., 1968. Study on uplift resistance of footing (II). Soils and Foundations 8 (4), 18–48.

Merifield, R.S., Sloan, S.W., 2006. The ultimate pullout capacity of anchors in frictional soils. Canadian Geotechnical Journal 43 (8), 852–868.

Meyerhof, G.G., Adams, J.I., 1968. The ultimate uplift capacity of foundations. Canadian Geotechnical Journal 5 (4), 225–244.

Meyerhof, G.G., 1973. The uplift capacity of foundation under oblique load. Canadian Geotechnical Journal 10 (64), 64–70.

Miyata, Y., Bathurst, R.J., Konami, T., 2011. Evaluation of two anchor plate capacity models for MAW systems. Soils and Foundations 51 (5), 885–895.

Murray, E.J., Geddes, J.D., 1987. Uplift of anchor plates in sand. Journal of Geotechnical Engineering, ASCE 113 (3), 202–215.

Nimbalkar, S., Choudhury, D., 2007. Sliding stability and seismic design of retaining wall by pseudo-dynamic method for passive case. Soil Dynamics and Earthquake Engineering 27 (6), 497–505.

Rangari, S., Choudhury, D., Dewaikar, D.M., 2011a. Pseudo-static uplift capacity of horizontal strip anchor. In: Han, J., Alzamora, D.E. (Eds.), Geo-Frontiers 2011: Advances in Geotechnical Engineering. Geotechnical Special Publication No. 211, ASCE, Reston, VA, USA, pp. 1821–1831.

Rangari, S., Choudhury, D., Dewaikar, D.M., 2011b. Pseudo-static uplift capacity of inclined strip anchor in cohesionless soil. Electronic Journal of Geotechnical Engineering 16, 1185–1200.

Rangari, S., Choudhury, D., Dewaikar, D.M., 2013. Computations of seismic passive resistance and uplift capacity of horizontal strip anchors in sand. Geotechnical and Geological Engineering 31 (2), 569–580.

Richards, R., Elms, D.G., Budhu, M., 1990. Dynamic fluidization of soils. Journal of Geotechnical Engineering, ASCE 116 (5), 740–759.

Rowe, R.K., Davis, E.H., 1982. The behaviour of anchor plates in sand. Geotechnique 32 (1), 25–41.

Steedman, R.S., Zeng, X., 1990. The influence of phase on the calculation of pseudo-static earth pressure on a retaining wall. Geotechnique 40 (1), 103–112.

Subba Rao, K.S., Choudhury, D., 2005. Seismic passive earth pressures in soils. Journal of Geotechnical and Geoenvironmental Engineering 131 (1), 131–135.

Subba Rao, K.S., Kumar, J., 1994. Vertical uplift capacity of horizontal anchors. Journal of Geotechnical Engineering 120 (7), 1134–1147.

Tagaya, K., Tanaka, A., Aboshi, H., 1983. Application of finite element method to pullout resistance of buried anchor. Soils and Foundations 23 (13), 91–104.

Tagaya, K., Scott, R.F., Aboshi, H., 1988. Pullout resistance of buried anchor in sand. Soils and Foundations 28 (13), 114–130.

Vesic, A.S., 1971. Breakout resistance of objects embedded in ocean bottom. Journal of Soil Mechanics and Foundation Engineering Division, American Society of Civil Engineers 97 (9), 1183–1205.